Experimental results of HDR-TEMR thermal stratification test in horizontal feedwater lines

L.Wolf
Kernforschungszentrum Karlsruhe GmbH, Project HDR, FR Germany
U.Schygulla
Battelle-Institut e.V., Frankfurt am Main, FR Germany

1 INTRODUCTION

In recent years a particular form of crack formation has occurred in a number of BWRs and PWRs, Miksch et al (1985), at the internal surfaces of horizontal feedwater piping upstream of the reactor pressure vessels or steam generators, respectively.

Under low power conditions and hot standby or during startup and shutdown processes the feedwater mass flow is reduced to a few percent of the rate at full power. Under such conditions stratified flow develops and leads to the formation of a rather thin, separating mixing layer between the cold and hot fluid regions; its height depends primarily on the mass flow, the exit condition and the density ratio. This phenomenon of temperature stratification was confirmed by numerous in - service measurements in both PWR- and BWR-plants and in laboratory test models. Whereas in-plant measurements are primarily hampered by lack of instrumentation in the fluid and at the inside pipe surface, the scaled down laboratory experiments mostly resorted to simulating fluids under atmospheric conditions in transparent facilities leaving the question about proper extrapolation towards protoyypical conditions. To obtain more detailed and consistent sets of experimental data for fluid and inside/outside pipe wall surface temperatures to assess the effects of thermal shock, stratification and striping loads combination conditions, a series of experiments, TEMR, T33, has been performed at the HDR facility as described by Schygulla and Wolf (1986) under close to realistic conditions.

2 TEST MATRIX, EXPERIMENTAL FACILITY AND INSTRUMENTATION

In order to comply with all of the major issues of the test objectives for both BWR and PWR conditions a total of 25 experiments has been performed which can be grouped into the following categories:

1. Experiments T33.1 through T33.13: BWR conditions
2. Experiments T33.14 through T33.19+25: PWR conditions

The range of system pressure examined was between 1 to 40 bar with the cold water inlet temperature always kept at 30^{o}C and the initial hot fluid temperature ranging between 100^{o} C and 250^{o} C according to the system pressure. This spectrum of experimental conditions was anticipated to result in cold fluid heights between 0.1 and close to 0.4 m as specified by Schygulla and Wolf (1986).

Fig. 1 shows the isometry of the piping system and components. The inside diameter of the horizontal pipe is 397 mm; its length is 6 m. Along its length several measurement sections have been inserted as shown schematically in Fig. 2. As indicated the pressure vessel nozzle is protected by a thermal sleeve potruding into the horizontal pipe. At its exit, an orifice manipulator has been installed which is shown in detail in Fig. 3. Fig. 4 depicts the respective oblong with the orifices used for performing either the BWR-related experiments or hot water pocket tests. The PWR-related experiments have been performed without any orifice.

Fig. 5 gives a schematic overview of the axial, radial and azimuthal thermocouple positions in the primary measurement pipe section I (compare Fig. 2). One angular segment has been especially densely instrumented in order to get optimal resolution of hydraulic and thermal characteristics of the mixing layer. A triplet is positioned every 2.5^{o} from 90 to 105^{o} over this segment. Fig. 6 depicts the circumferential distribution of pairs of azimuthal/axial strain gages.

3 EXPERIMENTAL RESULTS AND COMPARISONS WITH BLIND PRE-TEST PREDICTIONS

In the following, experimental data for the BWR-test, T33.9, and the PWR-test T33.19 will be shown. Both experiments are characterized by about the same height of the cold fluid layer in the region of densely applied instrumentation. The initial conditions were as follows:

<u>T33.9:</u> P = 40 bar; $T_H = 250^{o}$ C; $T_c = 30^{o}$ C; $V = 0.0078\ m^3/s$

<u>T33.19:</u> P = 20 bar; $T_H = 212^{o}$ C; $T_c = 30^{o}$ C; $V = 0.013\ m^3/s$.

Fig. 7 shows pairs of consistent figures for the transient fluid, pipe surface inside and outside temperatures for the BWR-experiment T33.9 and PWR-experiment T33.19, respectively. The following observations can be made from the individual graphs of Fig. 7 and comparisons among them:

1. Prior to the onset of thermal shock precursory cooldown due to azimuthal conduction leads to a temperature decrease.

2. The rather instantaneous thermal shock is accompanyed by large temperature fluctuations; the fluctuations deem larger for the PWR-type experiment, for both experiments they last over the total experimental time; no damping effects exist between sold leg center and wall regions.

3. The mixing layer deems confined between 95^{o} and 100^{o} for T33.9 (BWR) whereas it seems much broader for T33.19 (PWR).

4. The inside surface temperatures show fluctuations (BWR: 0.7 Hz) whose amplitudes are reduced by about 30%; by boundary layer and conductive effects; still the remaining amplitudes for T33.19 are in the order of 30^{o}C whereas for T33.9 these are reduced to about 8^{o}C.

5. Radial and azimuthal conduction effects in the pipe wall lead to a complete dampening of the fluctuations at the outside pipe surface for both experiments.

6. Careful examinations of the three types of temperature traces reveal that for positions between 90^{o} and 105^{o} surface temperatures are below the fluid temperature for both types of experiments due to azimuthal heat conduction effects. This can be more clearly seen from Fig. 8 which shows the superposition of the temperatures at 90^{o}.

This leads to the following far reaching conclusions for the conditions shown in these graphs:

1. There is no simple, unique correspondence between outside temperature reading and fluid response and vice versa, i.e. on-line surveillance methods relying only on outside surface temperature readings cannot infer thermal fluid loads without resorting to rather complicated software and tuning.

2. Extrapolation from thermal fluid response in transparent model facilities towards real plants is not straightforward, if not even misleading because of the missing link between convective/conductive effects and their interdependencies as well as their use of sumulant fluids.

From the data as shown in Fig. 7 the bandwidths of the temperature fluctuations around final steady-state conditions are plotted over the region of pipe diameter of interest in Fig. 9 for T33.9 and T33.19, respectively. For about the same cold fluid layer height, the following conclusions may be drawn from these figures:

1. The fluctuating temperature region is broader (13 mm vs. 5 mm) for PWR than BWR conditions; waves can be clearly identified for PWR-tests.

2. The bandwidth of temperature fluctuations is somewhat larger for BWR (inferred from the graph) than PWR conditions in the critical position; waves are smeared out and can barely be identified for BWR-tests.

3. For PWR conditions the regions of substantial amplitudes extends well above and below the cold fluid layer height.

4. The total height of the transition layer (characterized by measured temperature fluctuations) is larger for PWR than BWR conditions; for BWR-tests fluctuations are small as expected, but for PWR larger.

5. Mixing effects under PWR conditions raise the lower and reduce the higher temperatures observed over this part of the pipe diameter compared to the BWR tests.

Comparison of the derived characteristics for the mixing layer with pre-test estimates based on classical instability theory show notece-able deviations for both experiments. Improvements deem necessary.

Fig. 10 shows the comparison of measured azimuthal temperature profiles at 60 and 600 seconds and a 3-D SOLA-PTS simulation at 60 s. The agreement in terms of gradient and cold water temperature is fairly good. Deviations can be explained in terms of a 30% difference between specified and measured cold fluid mass flow and temperature. In addition, a finer nodalisation in the upper pipe region deems appropriate in order to reduce premature mixing in the hotter fluid region. Fig. 11 compares the measured with the calculated axial strains by 2-D analytical means with the calculated azimuthal temperature variation by SOLA-PTS developed in a Fourier series.

REFERENCES

Miksch, M.; Lenz, E.; Löhberg, R.: Loading Conditions in Horizontal Feedwater Pipes of LWRs Influenced by Thermal Shock and Thermal Stratification Effects, Nucl. Eng. Des. 84 (1985), 179-187

Schygulla, U.; Wolf, L.: Design Report: Thermal Stratification Experiments in a Horizontal Piping Section, HDR-Test Group TEMR T33, PHDR-Working Report No. 3.495/86, Nov. 1986.

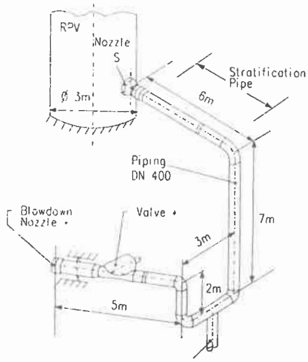

Fig.1: Isometry of HDR-TEMR Facility

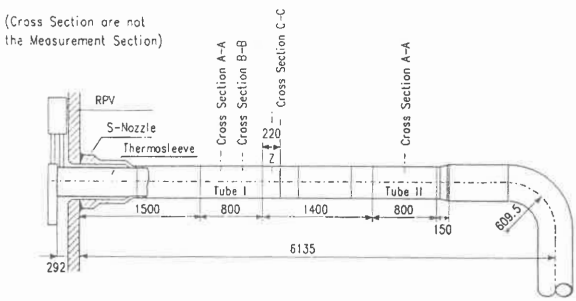

Fig.2: Overall Arrangement of TEMR Stratification Pipe With Thermal Sleeve, and Orifice Manipulator

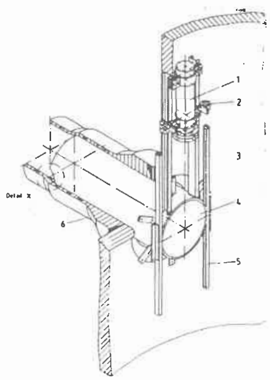

Fig.3: Orifice Manipulator

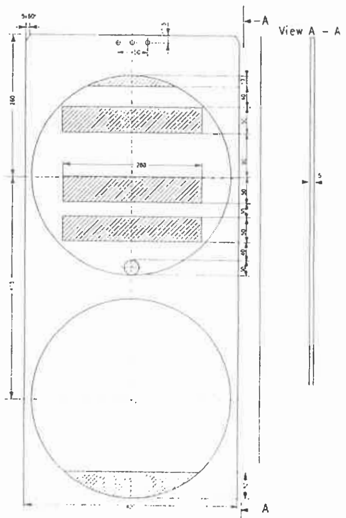

Fig.4: Oblong with BWR-Orifice (Top) and Hot Water Pocket Simulation Orifice (Bottom)

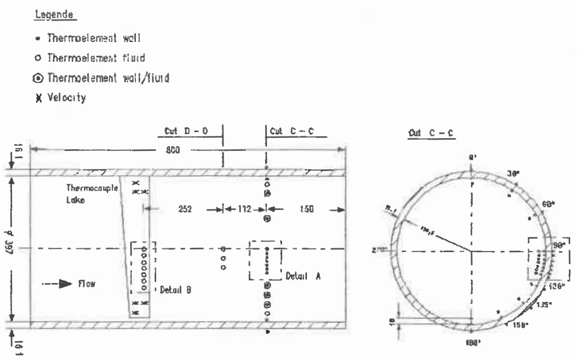

Fig.5: Axial and Radial Cross-Section Through TEMR Pipe

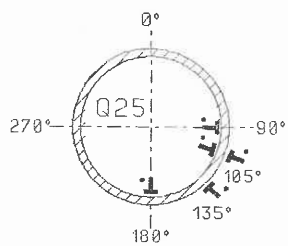

Fig.6: Azimuthal Strain Gage Positions

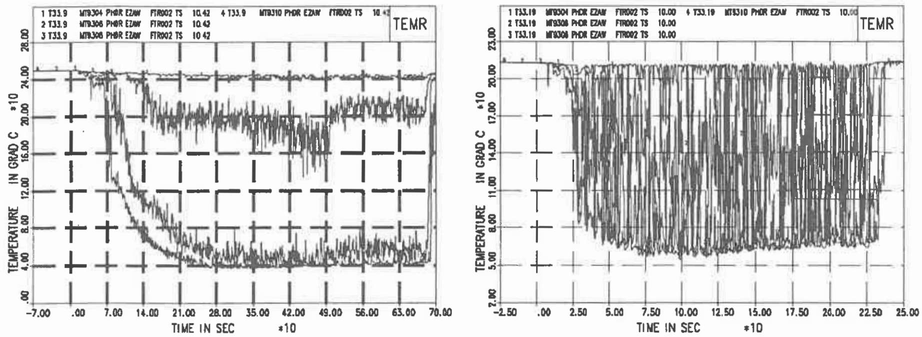

Fluid Temperatures Close to Wall

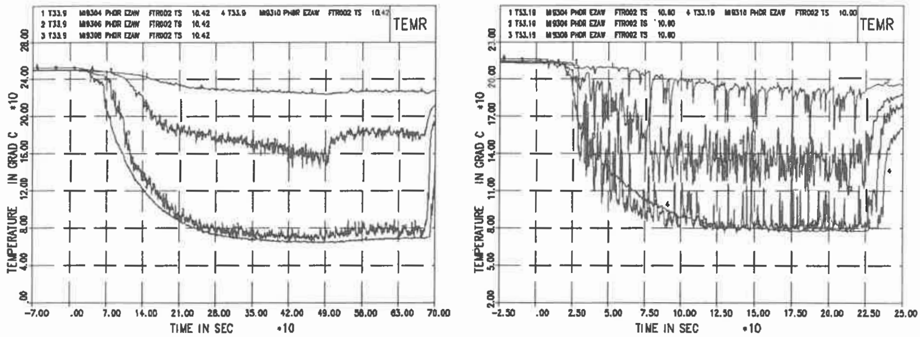

Pipe Inside Surface Temperatures

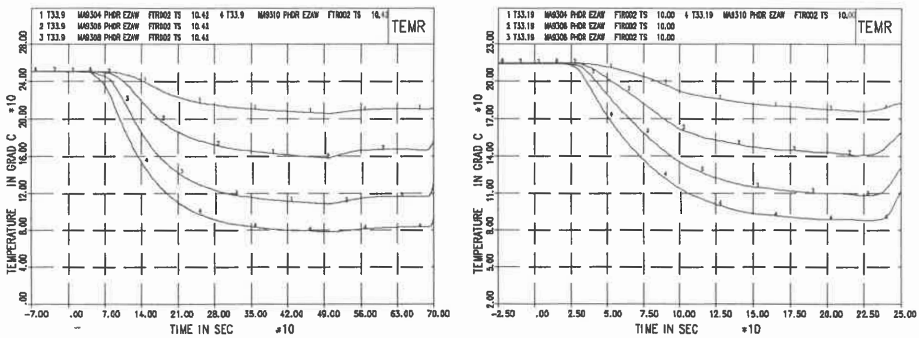

Pipe Outside Surface Temperatures

BWR: T33.9 **PWR: T33.19**

Fig.7: Transient Histories of Fluid and Pipe Surface Temperatures Between 90° and 105° of Pipe Circumference for BWR and PWR Type HDR-Experiments

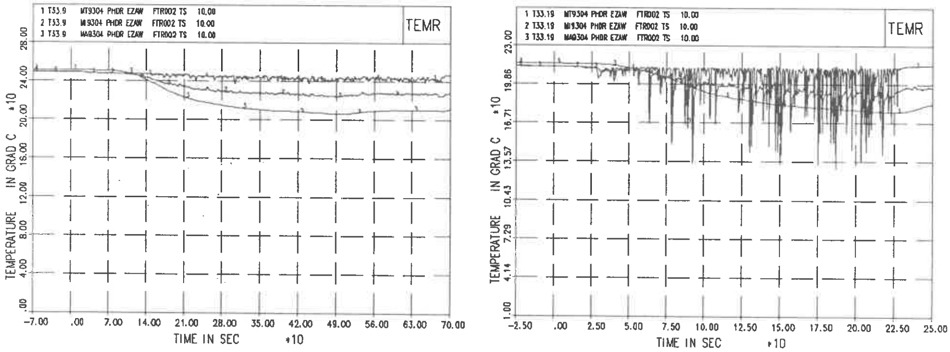

Fig. 8: Superposition of Transient Fluid and Pipe Surface Temperatures at 90° for BWR and PWR-typical HDR-Experiments

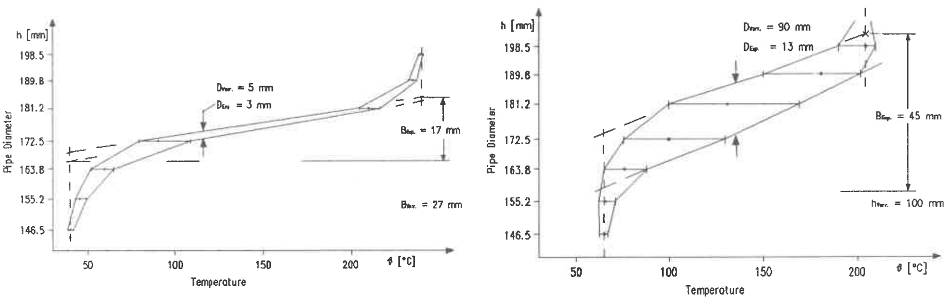

Fig. 9: Evaluated Cold Water Height and Transition Mixing Layer Characteristics from Temperature Fluctuations

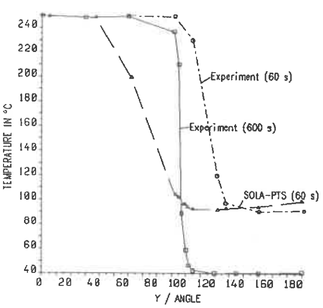

Fig. 10: Comparison of Measured and Calculated Temperature Profiles Around the Circumference

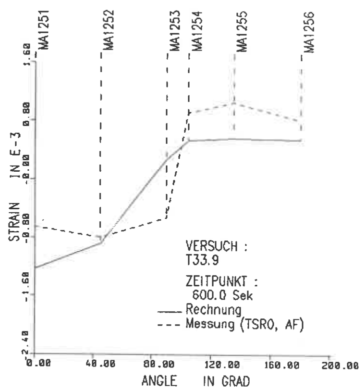

Fig. 11: Comparison of Measured and Calculated Axial Strain Profiles at the Pipe Outside Surface